

## Electron interaction-driven insulating ground state in Bi<sub>2</sub>Se<sub>3</sub> topological insulators in the two-dimensional limit

Minhao Liu,<sup>1</sup> Cui-Zu Chang,<sup>1,2</sup> Zuocheng Zhang,<sup>1</sup> Yi Zhang,<sup>2</sup> Wei Ruan,<sup>1</sup> Ke He,<sup>2,\*</sup> Li-li Wang,<sup>2</sup> Xi Chen,<sup>1</sup> Jin-Feng Jia,<sup>1</sup> Shou-Cheng Zhang,<sup>3,4</sup> Qi-Kun Xue,<sup>1,2</sup> Xucun Ma,<sup>2</sup> and Yayu Wang<sup>1,†</sup>

<sup>1</sup>Laboratory of Low Dimensional Quantum Physics, Department of Physics, Tsinghua University, Beijing 100084, People's Republic of China

<sup>2</sup>Institute of Physics, Chinese Academy of Sciences, Beijing 100190, People's Republic of China

<sup>3</sup>Department of Physics, Stanford University, Stanford, California 94305-4045, USA

<sup>4</sup>Institute for Advanced Study, Tsinghua University, Beijing 100084, People's Republic of China

(Received 18 February 2011; published 26 April 2011)

We report a transport study of ultrathin Bi<sub>2</sub>Se<sub>3</sub> topological insulators with thickness from one quintuple layer to six quintuple layers grown on sapphire by molecular beam epitaxy. At low temperatures, the film resistance increases logarithmically with decreasing temperature, revealing an insulating ground state. The insulating behavior becomes more pronounced in thinner films. The sharp increase of resistance with magnetic field, however, indicates the existence of weak antilocalization originated from the topological protection. We show that this unusual insulating ground state in the two-dimensional limit of topological insulators is induced by the combined effect of strong electron interaction and topological delocalization.

DOI: [10.1103/PhysRevB.83.165440](https://doi.org/10.1103/PhysRevB.83.165440)

PACS number(s): 73.61.Le, 73.20.Fz, 73.50.Jt

### I. INTRODUCTION

Topological insulators (TI) are a new class of insulators with topologically nontrivial band structures originated from strong spin-orbit coupling (SOC).<sup>1–3</sup> The discovery of quantized spin Hall effect (QSHE) in two-dimensional (2D) TI<sup>4,5</sup> stimulated intensive search for new TI systems and associated novel phenomena. Recently, three-dimensional (3D) TIs have been predicted and experimentally verified in a series of compounds exemplified by Bi<sub>1–x</sub>Sb<sub>x</sub>,<sup>6,7</sup> Bi<sub>2</sub>Se<sub>3</sub>, Bi<sub>2</sub>Te<sub>3</sub>, and Sb<sub>2</sub>Te<sub>3</sub>.<sup>8,9</sup> These materials possess an insulating energy gap in the bulk and gapless surface state (SS) protected by time-reversal symmetry. The topologically protected SSs have been proposed to host a variety of exotic magnetoelectric phenomena including Majorana fermions,<sup>10</sup> magnetic monopole,<sup>11</sup> and quantized anomalous Hall effect.<sup>12</sup>

Many unique features of the TI SSs, such as Dirac-like linear band dispersion,<sup>8,13,14</sup> chiral spin texture,<sup>15</sup> absence of backscattering,<sup>16–18</sup> and Landau level quantization,<sup>19,20</sup> have been revealed by surface-sensitive probes including angle-resolved photoemission spectroscopy (ARPES) and scanning tunneling microscopy (STM). The transport properties of the SSs, however, are often mixed with those from the bulk states because it is difficult to grow bulk insulating samples. This has been a main hurdle for realizing the proposed novel phenomena and applications of TIs. Reduction of bulk carriers has been achieved by doping or annealing<sup>21–23</sup> of bulk crystals and gate tuning of nanostructures.<sup>24,25</sup> Fabricating ultrathin TI films represents another effective approach to reduce bulk conduction by enhancing the surface-to-volume ratio. This method also allows us to tune the coupling of the two surfaces to reach the 2D limit of TIs,<sup>26–28</sup> which has been proposed to exhibit QSHE<sup>26</sup> and enhanced thermoelectric performance.<sup>29</sup> The localization behavior in this regime also attracted tremendous interests because it belongs to the symplectic class with a topological term.<sup>30–34</sup> However, transport properties in the 2D regime of 3D TIs have not been experimentally investigated in a systematic manner.

Molecular beam epitaxy (MBE) has proved a powerful technique for fabricating high-quality ultrathin TI films down to a few quintuple layers (QLs).<sup>28,35</sup> In this paper we report electrical transport studies on Bi<sub>2</sub>Se<sub>3</sub> films with precisely controlled layer thickness from 1 QL to 6 QLs. At sufficiently low temperatures, the film resistance shows a logarithmic divergence, indicating an insulating ground state. The weak-field magnetoresistance (MR), on the contrary, always shows a positive cusp characteristic of weak antilocalization (WAL). We propose that this unusual insulating ground state in the 2D limit of TIs is induced by the combined effect of strong electron interaction and topological delocalization. The relevance of electron interactions revealed here suggests that TIs may exhibit exotic many-body effects beyond the framework of single-particle band theory.

### II. EXPERIMENTAL

The ultrathin Bi<sub>2</sub>Se<sub>3</sub> films studied here are grown on sapphire substrate by molecular beam epitaxy, as described in detail elsewhere.<sup>36</sup> The structure and thickness of the films are monitored *in situ* by reflection high-energy electron diffraction (RHEED). The quality of the sample can be seen from the STM image of a 4-QL film shown in Fig. 1(a). Except for nanoscale 1-QL-high voids and plateaus, the film is atomically flat on macroscale. After the growth of a Bi<sub>2</sub>Se<sub>3</sub> film, 20 nm of highly insulating amorphous Se layer is deposited on top of it to prevent the film from direct exposure to air. Ti/Au electrodes are then deposited on the sample, forming millimeter-sized transport devices as schematically shown in Fig. 1(b).

The longitudinal and transverse electrical transport properties of the Bi<sub>2</sub>Se<sub>3</sub> films are measured by using standard four-probe ac lock-in method. The total 2D carrier density estimated from the Hall coefficient is  $n_{2D} = (3.5 \pm 0.5) \times 10^{13} / \text{cm}^2$ , which varies slightly with the film thickness. ARPES measurements on the same films reveal well-defined SSs with Fermi wave vector  $k_F \sim 0.1 \text{ \AA}^{-1}$ .<sup>36</sup> The total SS carrier density can thus be calculated to be  $n_{2D} \sim 3.2 \times 10^{13} / \text{cm}^2$  ( $n_{2D} \sim 1.6 \times 10^{13} / \text{cm}^2$

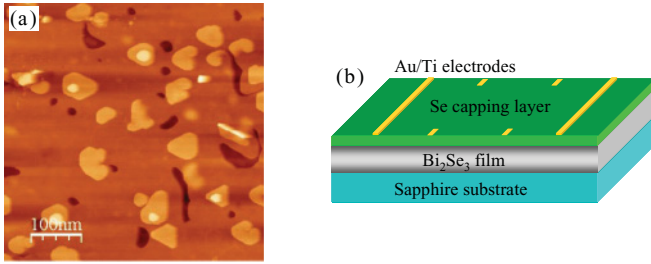


FIG. 1. (Color online) (a) An *in situ* STM image of a  $\text{Bi}_2\text{Se}_3$  film with thickness  $d = 4$  QL. The film is flat on macroscale, except for nanoscale islands and voids with 1 QL thickness. (b) Schematic structure of the  $\text{Bi}_2\text{Se}_3$  ultrathin film for transport measurements (the thickness is not to scale).

for each surface). Therefore, the majority of the carriers come from the SSs, and the dominance of SS charge transport in this regime is justified.

### III. RESULTS AND DISCUSSION

Figure 2 shows the 2D sheet resistance ( $R_{\square}$ ) vs temperature ( $T$ ) for ultrathin  $\text{Bi}_2\text{Se}_3$  films with thicknesses  $d = 1$  to 6 QLs. The 1-QL film is highly insulating with  $R_{\square}$  much larger than the quantum resistance  $h/e^2$ . This is most likely due to the poor interface between the first Se layer and the sapphire substrate

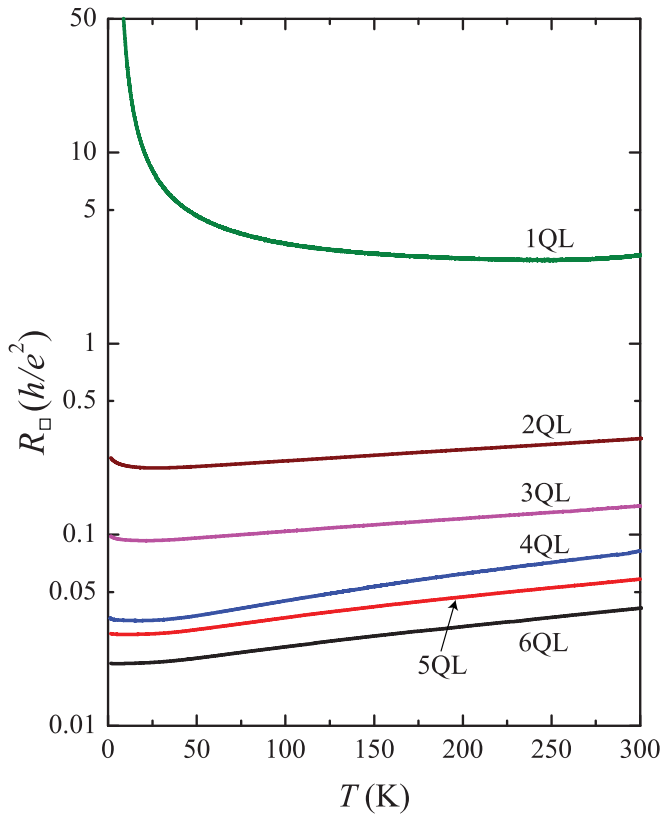


FIG. 2. (Color online) The  $R_{\square}$  vs  $T$  curves for  $\text{Bi}_2\text{Se}_3$  with thickness  $d = 1$  to 6 QL. The resistance value decreases systematically with increasing film thickness. Films with thickness  $d \geq 2$  QL display metallic behavior at high temperatures but become insulating at sufficiently low temperatures.

caused by the large lattice mismatch. As  $d$  is increased to 2 QLs, the  $R_{\square}$  value drops quickly to a fraction of  $h/e^2$ , indicating much improved film quality. As  $d$  increases further,  $R_{\square}$  keeps dropping, mainly due to the enhanced electron mobility. The mobility at  $T = 2$  K is estimated to be  $31 \text{ cm}^2/\text{V s}$  for the 2-QL film and  $350 \text{ cm}^2/\text{V s}$  for the 6-QL film. For all the films between 2 and 6 QLs, the  $R_{\square}$  vs  $T$  curves show metallic (with positive slopes) behavior at high temperatures. At sufficiently low temperatures, however, the  $R_{\square}$  reaches a minimum value and then increases with decreasing  $T$ , indicating the existence of an insulating ground state.

To elucidate the origin of the resistance upturn at low  $T$ , we renormalize the temperature dependence of  $R_{\square}$  by the minimum resistance and display it in logarithmic scale in Fig. 3(a). As indicated by the broken line, the  $R_{\square}$  of the 2-QL film increases logarithmically at low  $T$ . As the film thickness increases, the same behavior persists, although the slope of the logarithmic upturn keeps decreasing. Moreover, the  $T$  at which  $R_{\square}$  reaches the minimum, designated as  $T_{\min}$  hereafter, also decreases continuously as the film thickness increases. Both observations indicate that the insulating tendency is much stronger in thinner films. Figure 3(b) summarizes the  $T_{\min}$  of all the samples. A monotonic increase of  $T_{\min}$  with reducing thickness is clearly demonstrated.

Figure 4 displays the normalized MR of different films measured at  $T = 1.5$  K in a perpendicular magnetic field. The overall pattern of the MR curves evolves systematically with film thickness. In the 2-QL film, MR shows a steep increase at low field and starts to saturate at around 10 T. The magnitude of MR drops considerably in the 3-QL film, but the qualitative behavior remains the same. As  $d$  is further increased to above 4 QLs, the zero field cusp is still present, but confined to a progressively narrower field scale. In the high field regime the MR evolves into a parabolic  $H$  dependence. The parabolic contribution becomes larger in thicker films, reflecting the increased weight of bulk MR, which is known to be large, positive, and parabolic to  $H$ . The wiggles on the MR curves are not noises, but retraceable signals reminiscent of the conductance fluctuations found in  $\text{Bi}_2\text{Se}_3$  single crystals.<sup>21</sup>

The sharp increase of weak-field MR has been observed in single crystals,<sup>21</sup> nanoribbons,<sup>37</sup> and thin films<sup>24,38</sup> of TIs. The chiral spin structure of the topological SS breaks the spin-rotational symmetry. The localization thus belongs to the symplectic class and exhibits WAL. When an external magnetic field is applied perpendicular to the film, the WAL is suppressed by  $H$ , leading to a positive MR. The WAL behavior in TI is drastically different from that of conventional SOC materials, as will be discussed later. However, the MR is determined mainly by symmetry, thus can still be described by the Hikami-Larkin-Nagaoka (HLN) theory.<sup>39</sup> The HLN formula for weak-field conductance variation in the 2D limit is

$$\begin{aligned} \delta\sigma &= \sigma(B) - \sigma(0) \\ &= -\frac{\alpha e^2}{2\pi^2\hbar} \left[ \ln\left(\frac{\hbar}{4eBl_{\phi}^2}\right) - \psi\left(\frac{1}{2} + \frac{\hbar}{4eBl_{\phi}^2}\right) \right]. \end{aligned} \quad (1)$$

Here  $l_{\phi}$  is the phase coherence length,  $\psi$  is the digamma function, and  $\alpha$  is a coefficient equals to  $-1/2$  in the symplectic case.

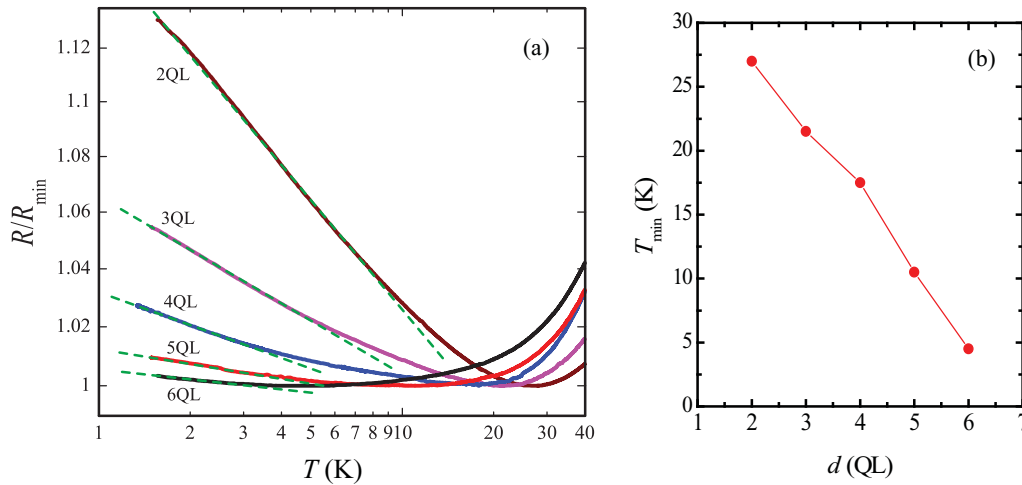


FIG. 3. (Color online) (a) The normalized  $R_{\square}$  shows a logarithmic increase with decreasing  $T$  (the broken lines are guides to the eyes). Both the slope of the logarithmic upturn and the  $T_{\min}$  increase with reducing  $d$ , indicating stronger insulating behavior in thinner films. (b) The thickness dependence of the resistivity minimum temperature  $T_{\min}$ .

Shown in Fig. 5(a) are theoretical fits to the low field magnetoconductance ( $\delta\sigma$ ) of the 2-, 3-, 5-, and 6-QL films measured at  $T = 1.5$  K. The HLN formula gives an excellent fit to all the curves, which demonstrates the existence of WAL in the 2D limit of TIs. One systematic trend revealed here is the larger field scales, hence the shorter phase coherence length, in thinner films. Figure 5(b) summarizes the thickness dependence of the  $l_{\phi}$  value extracted from the HLN fit. It increases from around 75 nm in 2-QL film to more than 200 nm in the 6-QL film. The  $\alpha$  value ranges between  $-0.3$  and  $-0.6$ , in rough agreement with the symplectic case.

Although WAL has been observed in many materials with strong SOC,<sup>40</sup> the nontrivial topology of the TIs has dramatic consequence on its localization/delocalization behavior. The weak localization of 2D massless Dirac fermions has attracted tremendous interest since the discovery of graphene.<sup>41–43</sup>

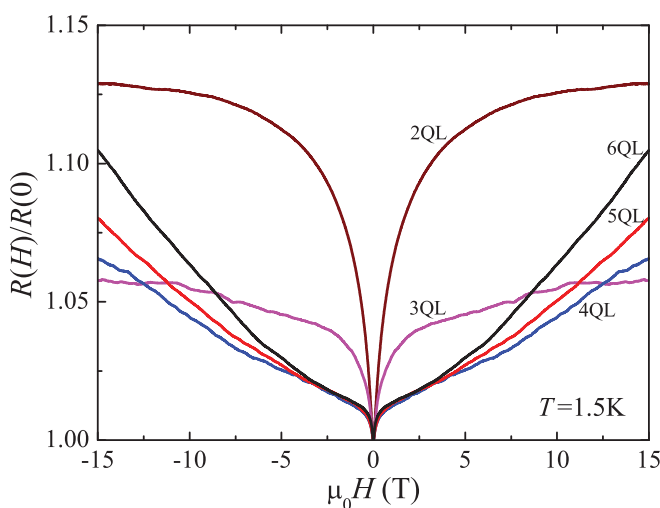


FIG. 4. (Color online) The magnetoresistance of the five films with  $d = 2$  to 6 QL all measured at  $T = 1.5$  K. In the weak  $H$  regime the MR shows a steep increase characteristic of WAL. For films with  $d \geq 4$  QL the contribution from the bulk states becomes pronounced in the high-field regime.

Scaling analysis shows that the massless Dirac fermions cannot be localized when intervalley scattering is absent, hence will remain metallic in the presence of arbitrarily strong disorder.<sup>30,43</sup> The underlying physical picture is that the Dirac fermions traveling along two time-reversed self-intersecting loops accumulate a  $\pi$  Berry phase, so backscattering is strictly prohibited due to the destructive quantum interference. This topological delocalization leads to a supermetallic “topological metal” phase fundamentally different from the WAL in conventional SOC system, which always becomes insulating when the disorder exceeds a critical level.<sup>30</sup>

The localization property of graphene is complicated by the existence of intervalley scattering.<sup>44–46</sup> The surface of 3D TIs is a more ideal system to realize the “topological metal” phase because the SS has a single massless Dirac cone. The electronic ground state of the TI thin film is expected to exhibit the predicted supermetallic behavior.<sup>30</sup> However, our transport results shown above unambiguously demonstrate an insulating ground state in the 2D regime of TI. This represents

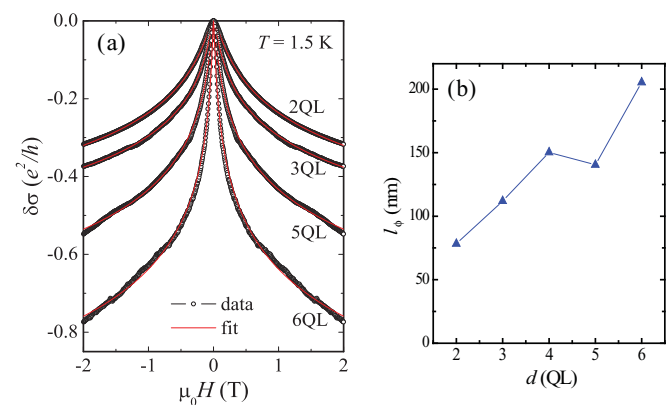


FIG. 5. (Color online) (a) The HLN fit of the weak-field  $\delta\sigma$  for films with different  $d$  measured at  $T = 1.5$  K. The thinner films have larger field scale, hence shorter phase coherence length, than the thicker films. (b) The thickness dependence of the phase coherence length  $l_{\phi}$ .

a gross departure from the single-electron, one-parameter scaling theory of Anderson localization.

We propose that the only possible explanation for this anomaly is the strong Coulomb interaction between electrons in the ultrathin TIs. As first realized by Altshuler and Aronov (AA),<sup>47</sup> the Coulomb repulsion in a 2D disordered metal is retarded due to the diffusive motion of charge carriers. Electron-electron interactions cannot be screened immediately and become strong and long-ranged. The enhanced interaction causes a suppression of electron density of state at the Fermi level and a logarithmic increase of resistivity with reducing  $T$ . In the  $\text{Bi}_2\text{Se}_3$  films studied here, the AA interaction effect and topological delocalization (TD) coexist and compete with each other. The total quantum correction to conductivity can be expressed as

$$\delta\sigma(T) = \delta\sigma_{TD}(T) + \delta\sigma_{AA}(T). \quad (2)$$

Here  $\delta\sigma_{TD}$  represents the increase of conductivity by TD, and  $\delta\sigma_{AA}$  represents the suppression of conductivity by electron interaction. The observation of an insulating state in ultrathin  $\text{Bi}_2\text{Se}_3$  suggests that the electron interaction effect dominates in the 2D limit of TIs.

The effect of electron interaction and TD on the mesoscopic transport properties of TIs has only been addressed recently,<sup>29,34</sup> and a quantitative treatment is still lacking. The 2D regime of 3D TIs turns out to be particularly rich and complex due to the hybridization between the wave functions of the top and bottom surfaces. As shown by ARPES measurements,<sup>28,36</sup> the coupling between the surfaces opens an energy gap at the Dirac point when the thickness of  $\text{Bi}_2\text{Se}_3$  is below 6 QLs, which is exactly the regime studied here. This coupling breaks the perfect topological protection of the SSs because now electrons can be scattered into the other surface (the situation is analogous to the intervalley scattering in graphene). A recent theory shows that in this regime the phase difference  $\delta\phi$  between two opposite loops (or the Berry phase) can be expressed as  $\delta\phi = \frac{\varepsilon^2 - \Delta_f^2}{\varepsilon^2} \pi$ .<sup>29</sup> Here  $\varepsilon$  is the energy of the SS electrons relative to the Dirac point and  $\Delta_f$  is the gap amplitude. Since the TD correction to conductance can be expressed as  $\delta\sigma_{TD}/\sigma = -\cos\delta\phi$ , this suggests that the conductance enhancement is much weakened in thinner film with larger  $\Delta_f$ . Using the  $\varepsilon$  and  $\Delta_f$  values measured by ARPES on the same films studied here,<sup>36</sup> we found that  $\delta\phi$  decreases from  $\pi$  in the 6-QL film to around  $0.6\pi$  in the 2-QL film, which means the relative conductance increase  $\delta\sigma_{TD}$  by TD is reduced from 100% in the 6-QL film to merely 30% in the 2-QL film. The weakened TD in thinner  $\text{Bi}_2\text{Se}_3$  films is a unique feature of the TIs in the 2D limit. In conventional SOC materials, the WAL effect usually becomes more pronounced as the system approaches the 2D regime due to the larger probability of forming self-intersecting loops.

The interaction effect, on the other hand, is enhanced in thinner films due to reduced dimensionality and increased disorder. Both effects lead to poorer screening, hence stronger Coulomb interaction between electrons. The shorter phase coherence length in thinner films [Fig. 5(b)] may partly be due to larger electron-electron scattering rate. The combined effect of enhanced interaction strength and weakened TD gives

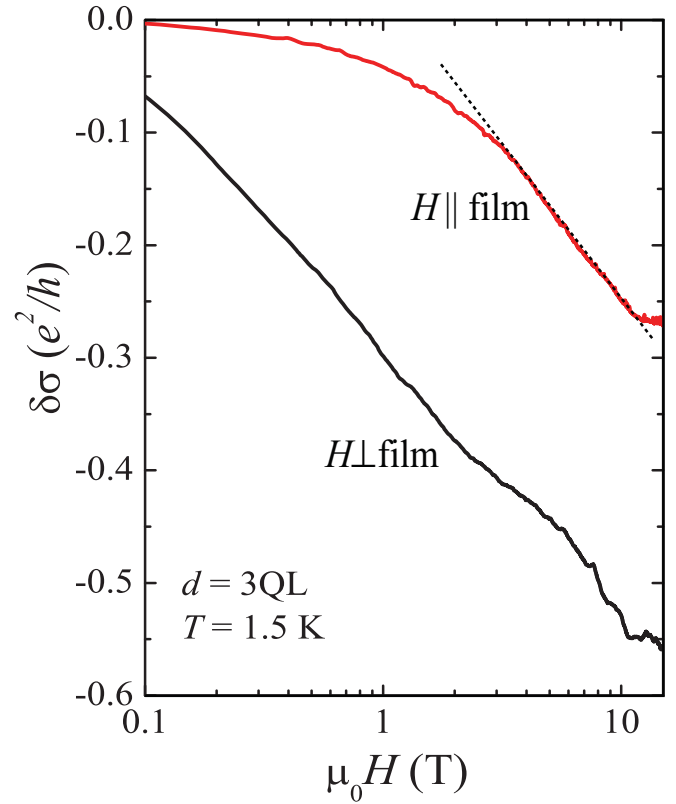


FIG. 6. (Color online) The variation of conductance of the 3-QL film for field parallel ( $\delta\sigma_{\parallel}$ , red) and perpendicular ( $\delta\sigma_{\perp}$ , black) to the film measured at  $T = 1.5$  K. Note that the field is in logarithmic scale. The broken line shows the logarithmic field dependence of parallel magnetoconductance, in agreement with the electron interaction picture.

a qualitative explanation of the stronger insulating property in thinner films.

The electron interaction effect also manifests itself in the field dependence of conductivity. In the AA interaction mechanism, spin splitting by external field leads to a decrease of conductivity with  $H$ . For  $h = g\mu_B H/k_B T \gg 1$ , that is, Zeeman splitting much larger than thermal activation,  $\delta\sigma_{AA}$  has a logarithmic  $H$  dependence:  $\delta\sigma_{AA}(H) = -\frac{e^2}{h} \frac{\tilde{F}_\sigma}{2\pi} \ln \frac{h}{1.3}$ ,<sup>48</sup> where  $\tilde{F}_\sigma$  is a number characteristic of the Coulomb interaction. Unlike the  $\delta\sigma(H)$  from WAL, which is an orbital effect only sensitive to perpendicular magnetic field,  $\delta\sigma_{AA}(H)$  is isotropic to  $H$ . Figure 6 shows the  $\delta\sigma_{\parallel}$  measured for  $H$  parallel to the 3-QL film (red), which has a sizable variation exclusively coming from the spin splitting  $\delta\sigma_{AA}(H)$  term. For  $H > 4$  T,  $\delta\sigma_{\parallel}$  indeed has a  $\log H$  dependence, as indicated by the broken line. The fit using the AA formula gives  $\tilde{F}_\sigma = 0.74$ , a reasonable value for a 2D interacting system which is expected to have  $\tilde{F}_\sigma \sim 1$ .<sup>48</sup> The existence of electron interactions in the ultrathin TIs is thus confirmed.

Recently, the effect of electron interactions on the localization behavior of the SSs of 3D TIs has been investigated theoretically.<sup>34</sup> It is found that the disordered SS is a supermetal in the absence of electron interaction, but becomes an insulator via a quantum critical point when electron interaction is sufficiently strong.<sup>34</sup> Our transport results on ultrathin  $\text{Bi}_2\text{Se}_3$

are qualitatively consistent with this picture, although the predicted quantum critical behavior has yet to be verified.

#### IV. CONCLUSION

In summary, we have performed systematic transport studies on ultrathin  $\text{Bi}_2\text{Se}_3$  topological insulator films. Contrary to the topologically protected supermetal phase predicted by the single-particle scaling theory, the ground state of these ultrathin TIs is found to be insulating. We propose that this unusual insulating behavior is induced by electron-electron interactions in the presence of disorders, which is corroborated by the logarithmic variation of magnetoconductance in parallel magnetic fields. The stronger insulating properties in thinner films can be explained qualitatively by the combined effect of stronger electron interaction and weakened topological

protection in the 2D regime of TIs. These results suggest that TIs in the 2D limit are intrinsically quantum many-body systems. The strong electron interactions in a topologically nontrivial 2D electron system may give rise to a wealth of new phenomena that were not captured in the single-particle band theory, which has been used predominantly in previous studies of TIs.

#### ACKNOWLEDGMENTS

We thank X. Dai, Z. Fang, N. P. Ong, E. Y. Shang, C. S. Tian, and Z. Y. Weng for helpful discussions. This work was supported by the National Natural Science Foundation of China, the Chinese Academy of Sciences, and the Ministry of Science and Technology of China (Grant No. 2009CB929400).

\*kehe@aphy.iphy.ac.cn

†yayuwang@tsinghua.edu.cn

<sup>1</sup>X. L. Qi and S. C. Zhang, *Phys. Today* **63**, 33 (2010).

<sup>2</sup>J. E. Moore, *Nature (London)* **464**, 194 (2010).

<sup>3</sup>M. Z. Hasan and C. L. Kane, *Rev. Mod. Phys.* **82**, 3045 (2010).

<sup>4</sup>B. A. Bernevig, T. L. Hughes, and S. C. Zhang, *Science* **314**, 1757 (2006).

<sup>5</sup>M. König, S. Wiedmann, C. Brune, A. Roth, H. Buhmann, L. W. Molenkamp, X. L. Qi, and S. C. Zhang, *Science* **318**, 766 (2007).

<sup>6</sup>L. Fu, C. L. Kane, and E. J. Mele, *Phys. Rev. Lett.* **98**, 106803 (2007).

<sup>7</sup>D. Hsieh, D. Qian, L. Wray, Y. Xia, Y. S. Hor, R. J. Cava, and M. Z. Hasan, *Nature (London)* **452**, 970 (2008).

<sup>8</sup>Y. Xia, D. Qian, D. Hsieh, L. Wray, A. Pal, H. Lin, A. Bansil, D. Grauer, Y. S. Hor, R. J. Cava, and M. Z. Hasan, *Nat. Phys.* **5**, 398 (2009).

<sup>9</sup>H. J. Zhang, C. X. Liu, X. L. Qi, X. Dai, Z. Fang, and S. C. Zhang, *Nat. Phys.* **5**, 438 (2009).

<sup>10</sup>L. Fu and C. L. Kane, *Phys. Rev. Lett.* **100**, 096407 (2008).

<sup>11</sup>X. L. Qi, R. Li, J. Zang, and S. C. Zhang, *Science* **323**, 1184 (2009).

<sup>12</sup>R. Yu, W. Zhang, H. J. Zhang, S. C. Zhang, X. Dai, and Z. Fang, *Science* **329**, 61 (2010).

<sup>13</sup>Y. L. Chen, J. G. Analytis, J. H. Chu, Z. K. Liu, S. K. Mo, X. L. Qi, H. J. Zhang, D. H. Lu, X. Dai, Z. Fang, S. C. Zhang, I. R. Fisher, Z. Hussain, and Z. X. Shen, *Science* **325**, 178 (2009).

<sup>14</sup>D. Hsieh, Y. Xia, D. Qian, L. Wray, J. H. Dil, F. Meier, J. Osterwalder, L. Patthey, J. G. Checkelsky, N. P. Ong, A. V. Fedorov, H. Lin, A. Bansil, D. Grauer, Y. S. Hor, R. J. Cava, and M. Z. Hasan, *Nature (London)* **460**, 1101 (2009).

<sup>15</sup>D. Hsieh, Y. Xia, L. Wray, D. Qian, A. Pal, J. H. Dil, J. Osterwalder, F. Meier, G. Bihlmayer, C. L. Kane, Y. S. Hor, R. J. Cava, and M. Z. Hasan, *Science* **323**, 919 (2009).

<sup>16</sup>P. Roushan, J. Seo, C. V. Parker, Y. S. Hor, D. Hsieh, D. Qian, A. Richardella, M. Z. Hasan, R. J. Cava, and A. Yazdani, *Nature (London)* **460**, 1106 (2009).

<sup>17</sup>T. Zhang, P. Cheng, X. Chen, J. F. Jia, X. C. Ma, K. He, L. L. Wang, H. J. Zhang, X. Dai, Z. Fang, X. Xie, and Q. K. Xue, *Phys. Rev. Lett.* **103**, 266803 (2009).

<sup>18</sup>Z. Alpichshev, J. G. Analytis, J. H. Chu, I. R. Fisher, Y. L. Chen, Z. X. Shen, A. Fang, and A. Kapitulnik, *Phys. Rev. Lett.* **104**, 016401 (2010).

<sup>19</sup>P. Cheng, C. Song, T. Zhang, Y. Zhang, Y. Wang, J. F. Jia, J. Wang, Y. Wang, B. F. Zhu, X. Chen, X. C. Ma, K. He, L. L. Wang, X. Dai, Z. Fang, X. Xie, X. L. Qi, C. X. Liu, S. C. Zhang, and Q. K. Xue, *Phys. Rev. Lett.* **105**, 076801 (2010).

<sup>20</sup>T. Hanaguri, K. Igarashi, M. Kawamura, H. Takagi, and T. Sasagawa, *Phys. Rev. B* **82**, 081305 (2010).

<sup>21</sup>J. G. Checkelsky, Y. S. Hor, M. H. Liu, D. X. Qu, R. J. Cava, and N. P. Ong, *Phys. Rev. Lett.* **103**, 246601 (2009).

<sup>22</sup>D. X. Qu, Y. S. Hor, J. Xiong, R. J. Cava, and N. P. Ong, *Science* **329**, 821 (2010).

<sup>23</sup>J. G. Analytis, R. D. McDonald, S. C. Riggs, J. H. Chu, G. S. Boebinger, and I. R. Fisher, *Nat. Phys.* **6**, 960 (2010).

<sup>24</sup>J. Chen, H. J. Qin, F. Yang, J. Liu, T. Guan, F. M. Qu, G. H. Zhang, J. R. Shi, X. C. Xie, C. L. Yang, K. H. Wu, Y. Q. Li, and L. Lu, *Phys. Rev. Lett.* **105**, 176602 (2010).

<sup>25</sup>J. G. Checkelsky, Y. S. Hor, R. J. Cava, and N. P. Ong, e-print arXiv:1003.3883v1 (to be published).

<sup>26</sup>C. X. Liu, H. J. Zhang, B. Yan, X. L. Qi, T. Frauenheim, X. Dai, Z. Fang, and S. C. Zhang, *Phys. Rev. B* **81**, 041307 (2010).

<sup>27</sup>H. Z. Lu, W. Y. Shan, Y. Wang, Q. Niu, and S. Q. Shen, *Phys. Rev. B* **81**, 115407 (2010).

<sup>28</sup>Y. Zhang, K. He, C. Z. Chang, C. L. Song, L. L. Wang, X. Chen, J. F. Jia, Z. Fang, X. Dai, W. Y. Shan, S. Q. Shen, Q. Niu, X. L. Qi, S. C. Zhang, X. C. Ma, and Q. K. Xue, *Nat. Phys.* **6**, 584 (2010).

<sup>29</sup>P. Ghaemi, R. S. K. Mong, and J. E. Moore, *Phys. Rev. Lett.* **105**, 166603 (2010).

<sup>30</sup>K. Nomura, M. Koshino, and S. Ryu, *Phys. Rev. Lett.* **99**, 146806 (2007).

<sup>31</sup>M. Onoda, Y. Avishai, and N. Nagaosa, *Phys. Rev. Lett.* **98**, 076802 (2007).

<sup>32</sup>S. Ryu, C. Mudry, H. Obuse, and A. Furusaki, *Phys. Rev. Lett.* **99**, 116601 (2007).

<sup>33</sup>K. I. Imura, Y. Kuramoto, and K. Nomura, *Phys. Rev. B* **80**, 085119 (2009).

<sup>34</sup>P. M. Ostrovsky, I. V. Gornyi, and A. D. Mirlin, *Phys. Rev. Lett.* **105**, 036803 (2010).

- <sup>35</sup>Y. Y. Li, G. Wang, X. G. Zhu, M. H. Liu, C. Ye, X. Chen, Y. Y. Wang, K. He, L. L. Wang, X. C. Ma, H. J. Zhang, X. Dai, Z. Fang, X. C. Xie, Y. Liu, X. L. Qi, J. F. Jia, S. C. Zhang, and Q. K. Xue, *Adv. Mater.* **22**, 4002 (2010).
- <sup>36</sup>C. Z. Chang, K. He, M. H. Liu, Z. C. Zhang, X. Chen, L. L. Wang, X. C. Ma, Y. Wang, and Q. K. Xue, SPIN (to be published).
- <sup>37</sup>H. Peng, K. Lai, D. Kong, S. Meister, Y. Chen, X. L. Qi, S. C. Zhang, Z. X. Shen, and Y. Cui, *Nat. Mater.* **9**, 225 (2010).
- <sup>38</sup>H. T. He, G. Wang, T. Zhang, I. K. Sou, J. N. Wang, H. Z. Lu, S. Q. Shen, and F. C. Zhang, e-print [arXiv:1008.0141v1](https://arxiv.org/abs/1008.0141v1) (to be published).
- <sup>39</sup>S. Hikami, A. I. Larkin, and Y. Nagaoka, *Prog. Theor. Phys.* **63**, 707 (1980).
- <sup>40</sup>G. Bergmann, *Phys. Rep.* **107**, 1 (1984).
- <sup>41</sup>E. McCann, K. Kechedzhi, V. I. Fal'ko, H. Suzuura, T. Ando, and B. L. Altshuler, *Phys. Rev. Lett.* **97**, 146805 (2006).
- <sup>42</sup>K. Nomura and A. H. MacDonald, *Phys. Rev. Lett.* **98**, 076602 (2007).
- <sup>43</sup>J. H. Bardarson, J. Tworzydło, P. W. Brouwer, and C. W. J. Beenakker, *Phys. Rev. Lett.* **99**, 106801 (2007).
- <sup>44</sup>A. F. Morpurgo and F. Guinea, *Phys. Rev. Lett.* **97**, 196804 (2006).
- <sup>45</sup>X. S. Wu, X. B. Li, Z. M. Song, C. Berger, and W. A. de Heer, *Phys. Rev. Lett.* **98**, 136801 (2007).
- <sup>46</sup>F. V. Tikhonenko, A. A. Kozikov, A. K. Savchenko, and R. V. Gorbachev, *Phys. Rev. Lett.* **103**, 226801 (2009).
- <sup>47</sup>B. L. Altshuler and A. G. Aronov, *Solid State Commun.* **30**, 115 (1979).
- <sup>48</sup>P. A. Lee and T. V. Ramakrishnan, *Rev. Mod. Phys.* **57**, 287 (1985).